ZS11)、鳥展示小屋４箇所 ZS1、ZS2、ZS8、ZS12)、ウサギ展示小屋３箇所（ZR1、ZR2、ZR3）と消毒後１箇所（ZS13)、ウサギ小屋近くの土壌１箇所（ZRCont)。

２：全菌数

EtBr 蛍光染色法で計測した。土壌希釈液をフィルターをセットしたろ過器にバファーを加え、さらに EtBr 水溶液を加える（終濃度 100μg／l)。室温で 10 分間放置後、吸引ろ過。ろ過滅菌水 3ml でフィルターを洗浄。無蛍光オイルで封入。検鏡計測。

３：好気培養による菌数計測

土壌懸濁液の 10 倍希釈系列 100μ l を環境微生物用の標準寒天培地２枚づつに接種した後、30℃において培養を行い、6 日後に菌数を測定した。

４：薬剤耐性菌

４－１）薬剤含有培地の作製

薬剤として ABPC(アミノベンジルペニシリン)、 SM(ストレプトマイシン)、EM(エリスロマイシン)、TC(テトラサイクリン)、OFLX(オフロキサシン)を用いた。環境細菌用標準培地を滅菌（オートクレーブ）した後、終濃度がそれぞれ 100 μg/ml、10 μg /ml、1 μg /ml となるよう添加した。

４－２）土壌微生物の培養方法

土壌希釈液 0.1ml を各濃度の薬剤入り培地に接種後、30 ℃で 40 時間培養した。対象群として薬剤の入っていない培地にも土壌希釈液 0.1ml を接種し、培養 40 時間後に各薬剤培地及び薬剤不含有培地のコロニー数を計測した。

４－３）薬剤耐性菌の検出率

40 時間培養後の薬剤耐性菌のコロニー数を、薬剤不含有培地のコロニー数を母数として割合を算出した。

Ⅱ．結果：

１：全菌数と好気培養による菌数計測

全菌数はいずれの土壌でも 1g 当たり 10^9～10^{10} 個であった。この結果は、処分場や山土、大学構内、畑などの結果と同じであった。

好気培養法で増殖する菌は、15 サンプルでは全菌数の 1～10%程度であった。しかし ZS1, ZS3, ZS5, ZS12 の 4 サンプルでは、それぞれ約 50%, 30%, 30%, 80%で、特に ZS12 は高い値を示した。

２：薬剤耐性菌

２－１：土壌別の薬剤耐性菌の検出率

・広場、ふれあい、動物飼育小屋に比べ、鳥飼育小屋で耐性菌の検出率が高い傾向が見られた。ノウサギ小屋で消毒後（ZS13）に検出率の顕著な増加が見られた。（図１）

- 各薬剤1μg/mlについては、図2にまとめた。ABPC, OFLX, EM. SM, TCの順に耐性菌が多かった。薬剤別に耐性菌（1μg/ml耐性）の割合が20%以上を超える土壌の数は、ABPC耐性を示す土壌が12箇所, OFLX 9箇所, EM 7箇所, SM 3箇所, TC 0箇所であった。
- 各薬剤10μg/mlについては、図3にまとめた。
- 各薬剤100μg/mlに対する耐性菌はほとんど検出されなかった。

図1:土壌別の耐性菌検出率

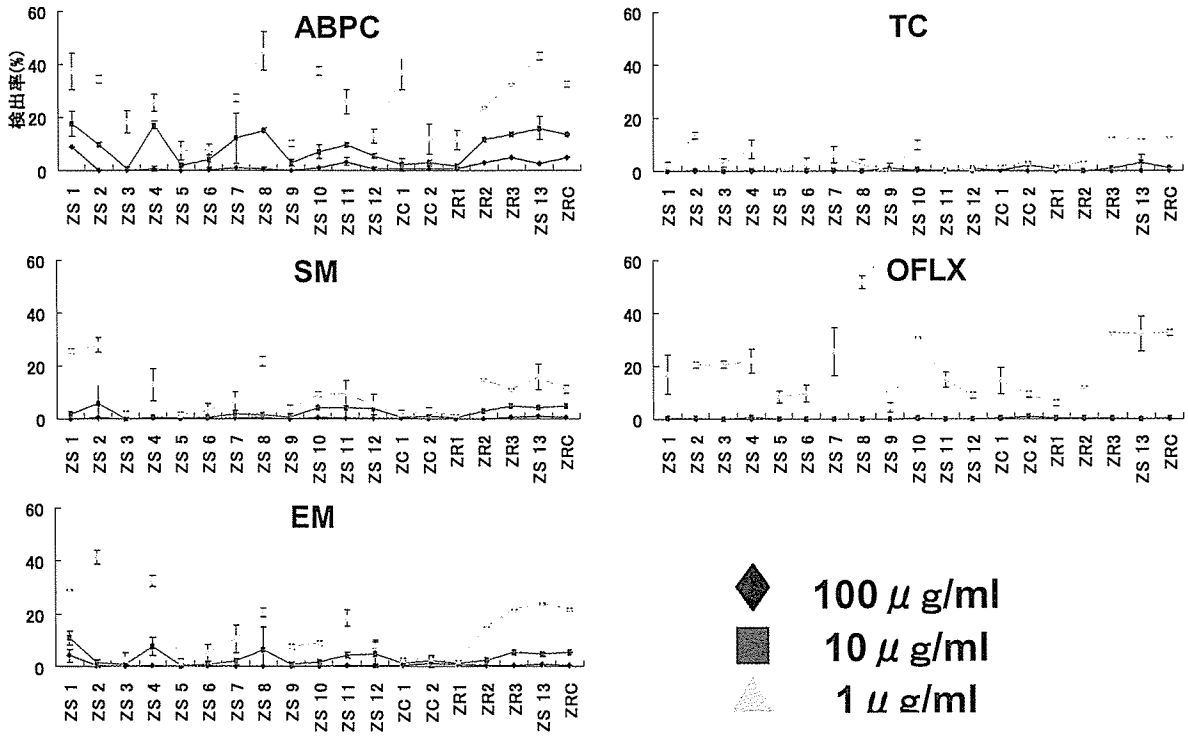

図2：各薬剤1μg/mlに対する耐性菌検出率

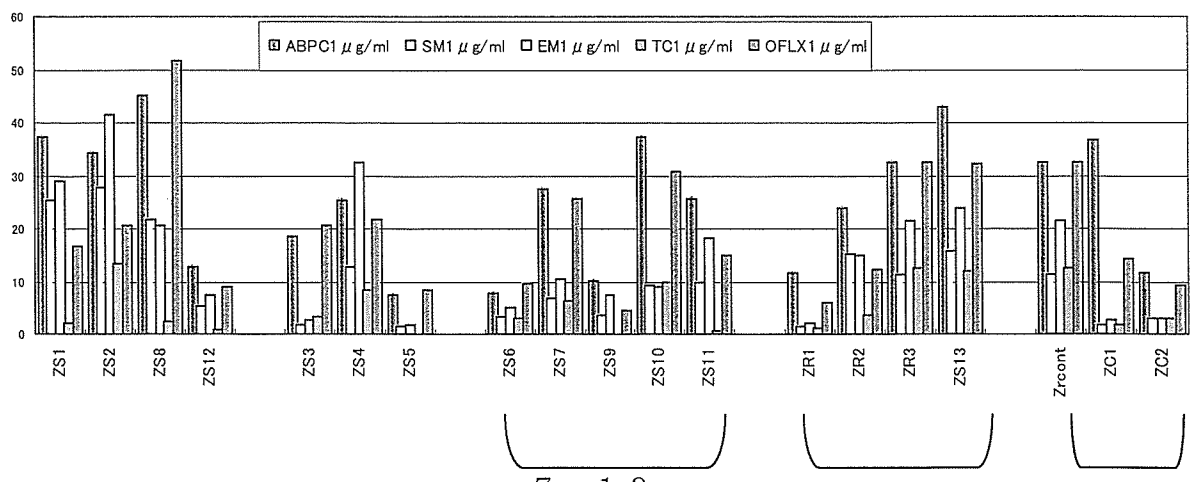

鳥　　ふれあい　　動物　　ノウサギ　　広場

2－2：土壌別の耐性菌の割合が 20%を超える薬剤の数（各薬剤 1μg/ml）

鳥展示小屋4箇所	0, 3, 4, 4	(ZS12, ZS1, ZS2, ZS8)
ふれあい広場3箇所	0, 1, 3	(ZS5, ZS3, ZS4)
動物展示小屋5箇所	0, 0, 1, 2, 2	(ZS6, ZS9, ZS11, ZS7, ZS10)
ノウサギ小屋4箇所	0, 1, 3, 3	(ZR1, ZR2, ZR3, ZS13)
広場など3箇所	0, 1, 3	(ZC2, ZC1, ZRcont)

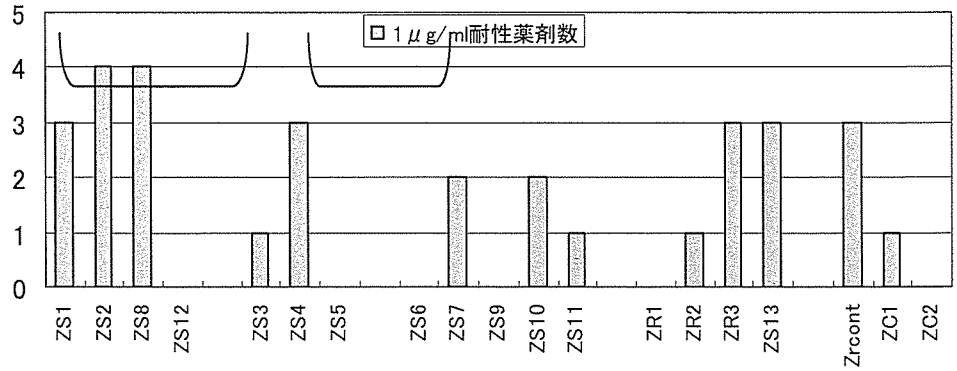

・1剤耐性は ABPC に、2剤耐性は ABPC と OFLX に、3剤耐性は ABPC,OFLX,EM に耐性を示した。

図 3：各薬剤 10μg/ml に対する耐性菌検出率

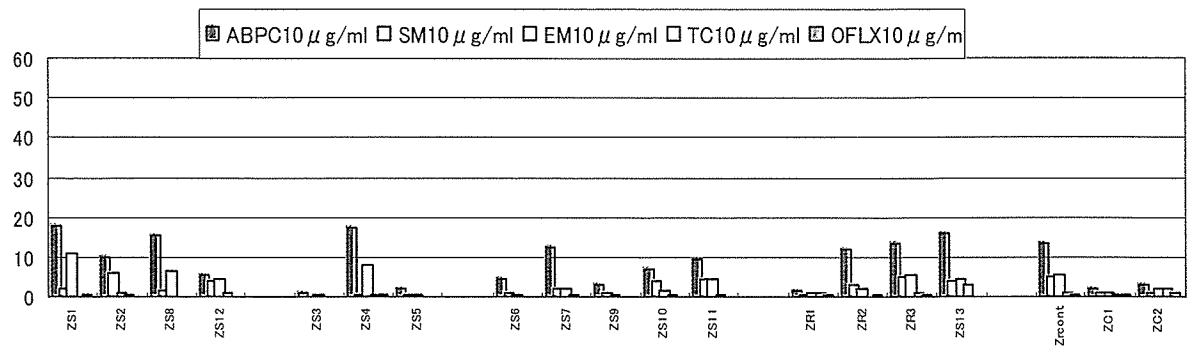

Ⅲ．まとめ

- 全菌数はいずれの土壌でも他の表層土壌と同様に 10^9～10^{10}/g であった。これは通常土壌の 1g 当たりの全菌数は、ほぼ一定に保たれているという、これまでの結果と一致するものであった。
- 好気培養法で増殖する菌数は、15 サンプルで全菌数の 1～10%程度であり、これも

- 通常土壌で得られる結果と一致していた。しかし、4サンプルでその割合が高い傾向が見られ、特に鳥類飼育小屋の ZS12 はその割合が全菌数の約 80%と他の土壌に比べて異常に高かった。原因として湿った土壌であったことが可能性として考えられた。感染症との関連は今後の検討課題である。
- 耐性菌の検出率は、土壌ごとに違いが見られた。
- 特に鳥類飼育小屋の ZS1, 2, 8 は TC 以外の 4 剤の耐性率が他のサンプルに比べ高い傾向であった。しかし鳥類飼育小屋であっても、ZS12 の場合は耐性率が低く、異なる傾向を示した。ZS12 は好気培養で増殖する菌の割合が異常に高く、母数が大きいために検出率が低かった可能性が考えられた。
- ノウサギ展示小屋の消毒前後(ZR1, 2, 13)を比較すると、消毒後の ZR13 は ABPC に耐性の割合が増加していた。消毒による菌種の選択が起きた可能性が考えられる。回復までの経時的検査が必要である。
- 耐性の割合は、昨年同様、ペニシリン系薬剤であるアミノベンジルペニシリンに対する耐性菌の検出率が最も高かった。これは 1μg/ml 耐性に顕著に見られた。グラム染色の結果、土壌の細菌はグラム陽性菌が多いにもかかわらず、ABPC 耐性菌の場合はグラム陰性桿菌が多かった。臨床上 ABPC 耐性は 8μg/ml 以上とされている。10μg/ml 以上の耐性を示す菌が 10%以上生息する土壌が 10 箇所であった（図 3)。自然界には ABPC 自然耐性の菌が多く生息している可能性と、本邦ではペニシリン系薬剤の使用頻度が最も高いことを反映している可能性も考えられた。
- ABPC の次に、OFLX, EM, SM の順に耐性率が高く、TC は最も低かった。
-

Ⅳ. 考察

動物展示場は、昨年の病院を併設している大学構内の土壌と同様に、耐性菌の占める割合が高かった。今回は 9 月の暑い時期に採取した、1 回だけの結果であるので、次年度は寒い時期のサンプル採取を行い、季節による違いを見る。また薬剤耐性菌だけでなく、菌種、菌叢の解析も行う予定である。

International Journal of Health Geographics

Methodology

A flexibly shaped spatial scan statistic for detecting clusters

Toshiro Tango and Kunihiko Takahashi

18 MAY 2005

BioMed Central

UK

International Journal of Health Geographics

BioMed Central

Methodology

Open Access

A flexibly shaped spatial scan statistic for detecting clusters

Toshiro Tango* and Kunihiko Takahashi

Address: Department of Technology Assessment and Biostatistics, National Institute of Public Health, 3-6 Minami 2 chome Wako, Saitama 351-0197 Japan

Email: Toshiro Tango* - tango@niph.go.jp; Kunihiko Takahashi - kunihiko@niph.go.jp

* Corresponding author

Published: 18 May 2005

Received: 14 April 2005

Accepted: 18 May 2005

International Journal of Health Geographics 2005, **4**:11 doi:10.1186/1476-072X-4-11

This article is available from: http://www.ij-healthgeographics.com/content/4/1/11

Abstract

Background: The spatial scan statistic proposed by Kulldorff has been applied to a wide variety of epidemiological studies for cluster detection. This scan statistic, however, uses a circular window to define the potential cluster areas and thus has difficulty in correctly detecting actual noncircular clusters. A recent proposal by Duczmal and Assunção for detecting noncircular clusters is shown to detect a cluster of very irregular shape that is much larger than the true cluster in our experiences.

Methods: We propose a flexibly shaped spatial scan statistic that can detect irregular shaped clusters within relatively small neighborhoods of each region. The performance of the proposed spatial scan statistic is compared to that of Kulldorff's circular spatial scan statistic with Monte Carlo simulation by considering several circular and noncircular hot-spot cluster models. For comparison, we also propose a new bivariate power distribution classified by the number of regions detected as the most likely cluster and the number of hot-spot regions included in the most likely cluster.

Results: The circular spatial scan statistics shows a high level of accuracy in detecting circular clusters exactly. The proposed spatial scan statistic is shown to have good usual powers plus the ability to detect the noncircular hot-spot clusters more accurately than the circular one.

Conclusion: The proposed spatial scan statistic is shown to work well for small to moderate cluster size, up to say 30. For larger cluster sizes, the method is not practically feasible and a more efficient algorithm is needed.

Background

The question of whether disease cases are clustered in space has received considerable attention in the literature [1-4]. Although many statistical tests for disease clusters have been proposed, most tests suffer from multiple testing problems due to one or two unknown parameters that must be set prior to their applications. For example, Cuzick and Edwards's procedure [5] has an unknown number k of nearest-neighbours and Besag and Newell's method [6] has an unknown number of cases k for the size of the cluster. As far as we know, the spatial scan statistic proposed by Kulldorff [7,8] and Tango's maximized excess events test [9,10] are exceptions and take multiple testing into account in the sense that we have only to specify the maximum possible cluster size. Especially, Kulldorff's circular spatial scan statistic has been applied to a wide

variety of epidemiological studies for cluster detection (for example, see [11-13]). In recent power comparisons of disease clustering tests, his scan statistic has been shown to be the most powerful for detecting localized clusters [14,15]. It should be noted, however, that the power estimates provided reflect the "power to reject the null hypothesis for whatever reason" and that the probability of both rejecting the null hypothesis and detecting the true cluster correctly is a different matter.

As the circular spatial scan statistic uses a "circular window" with variable size to define the potential cluster area, it is difficult to correctly detect noncircular clusters such as those along a river. Most geographical areas are noncircular. Furthermore, in our experience in applying SaTScan program [16] to various data, even if the null hypothesis is rejected, the circular spatial scan statistic tends to detect a larger cluster than the true cluster by absorbing surrounding regions where there is no elevated risk. It should be noted that although Kulldorff originally made no assumptions about the shape of the scanning window in his paper [8], a circular scanning window has been used in almost all purely spatial applications especially for the availability of software and computational speed.

Recently, Patil and Taillie [17] and Duczmal and Assunção [18] proposed non-circular spatial scan statistics based on the likelihood ratio test formulated in the same way as in the circular spatial scan statistic. To avoid undertaking computationally infeasible searches, they considered different approaches. Patil and Taillie [17] used the notion of "upper level set" to reduce the size of windows to be scanned and proposed "upper level set scan statistic". However, they do not discuss how to select the level g which defines the upper level set and do not provide any illustrations of their method nor any results of comparison with the circular scan statistic. Duczmal and Assunção [18], on the other hand, have applied a simulated annealing method in which they try to examine only the most promising windows using a graph-based algorithm to obtain the local maxima of a certain likelihood function over a subset of the collection of all the connected regions. Their method seems to be very complicated but they do not show any programmable procedure of their method. In our experience using their program (personal communication to Professor Duczmal via email) which is executable with the Borland C++ Builder 6, their scan statistic, in most cases, detected a cluster of peculiar shape that was much larger than the true cluster by absorbing not only surrounding regions with non-elevated risk but also faraway regions with non-elevated risk. An example of such properties of Duczmal and Assunção's procedure is shown later in comparison with the circular spatial scan statistic and the proposed flexible spatial scan statistic. That is why we did not include both the Patil and Taille method and Duczmal and Assunção's procedure in our simulation for comparison.

In this paper, we propose an alternative *flexibly shaped spatial scan statistic* ('flexible spatial scan statistic' hereafter) in which the detected cluster is allowed to be flexible in shape while at the same time the cluster is confined within relatively small neighborhoods of each region. The performance of the flexible spatial scan statistic is compared with that of the circular spatial scan statistic using Monte Carlo simulation. In comparing performance we examined not only the usual power but also the newly introduced bivariate power distribution classified by the number of regions detected as the most likely cluster and the number of hot-spot regions included in the most likely cluster. The proposed flexible spatial scan statistic is illustrated with some simulated disease maps for the Tokyo Metropolitan area.

Methods

Consider the situation where an entire study area is divided into m regions (for example, county, enumeration districts, etcetera). The number of cases in the region i is denoted by the random variable N_i with observed value n_i, $i = 1, ..., m$. Under the null hypothesis H_0 of no clustering, the N_i are independent Poisson variables such that

$$H_0 : E(N_i) = \xi_i,\ N_i \sim \text{Pois}(\xi_i),\ i = 1, ..., m \quad (1)$$

where Pois(e) denotes Poisson distribution with mean e and the ξ_i are the null expected number of cases in the region i. To specify the geographical position of each region, we will use the coordinates of the administrative population centroid.

Under this situation, the circular spatial scan statistic imposes a circular window Z on each centroid. For any of those centroids, the radius of the circle varies from zero to a pre-set maximum distance d or a pre-set maximum number of regions K to be included in the cluster. If the window contains the centroid of a region, then that whole region is included in the window. In total, a very large number of different but overlapping circular windows are created, each with a different location and size, and each being a potential cluster. Let Z_{ik}, $k = 1,..., K$, denote the window composed by the $(k - 1)$-nearest neighbours to region i. Then, all the windows to be scanned by the circular spatial scan statistic are included in the set

$$Z_1 = \{Z_{ik} \mid 1 \le i \le m,\ 1 \le k \le K\} \quad (2)$$

A flexible scan statistic we propose, on the other hand, imposes an *irregularly shaped* window Z on each region by connecting its adjacent regions. For any given region i, we

create the set of irregularly shaped windows with *length k* consisting of k connected regions including i and let k moves from 1 to the pre-set maximum K. To avoid detecting a cluster of *unlikely peculiar shape*, the connected regions are restricted as the subsets of the set of regions i and $(K - 1)$-nearest neighbours to the region i where K is a pre-specified maximum length of cluster. In total, as in the circular spatial scan statistic, a very large number of different but overlapping arbitrarily shaped windows are created. Let $\mathbf{Z}_{ik(j)}$, $j = 1,..., j_{ik}$ denote the j-th window which is a set of k regions connected starting from the region i, where j_{ik} is the number of j satisfying $\mathbf{Z}_{ik(j)} \subseteq \mathbf{Z}_{ik}$ for $k = 1,..., K$. Then, all the windows to be scanned are included in the set

$$Z_2 = \{\mathbf{Z}_{ik(j)} \mid 1 \le i \le m, 1 \le k \le K, 1 \le j \le j_{ik}\} \quad (3)$$

In other words, for any given region i, the circular spatial scan statistic consider K concentric circles, whereas the flexible scan statistic consider K concentric circles plus all the sets of connected regions (including the single region i) whose centroids are located within the K-th largest concentric circle. So, the size of Z_2 is far larger than that of Z_1 which is at most mK. Details of the algorithm that we adopted to find all these arbitrarily shaped windows within a pre-specified maximum length K are given in the Appendix.

Under the alternative hypothesis, there is at least one window $\mathbf{Z}$ for which the underlying risk is higher inside the window when compared with outside. In other words, we are considering the following hypothesis:

$$H_0 : E(N(\mathbf{Z})) = \xi(\mathbf{Z}), \text{ for all } \mathbf{Z}, \; H_1 : E(N(\mathbf{Z})) > \xi(\mathbf{Z}), \text{ for some } \mathbf{Z} \quad (4)$$

where $N()$ and $\xi()$ denote the random number of cases and the null expected number of cases within the specified window, respectively. For each window, it is possible to compute the likelihood to observe the observed number of cases within and outside the window, respectively. Under the Poisson assumption, the test statistic, which was constructed with the likelihood ratio test [8], is given by

$$\sup_{\mathbf{Z} \in Z} \left(\frac{n(\mathbf{Z})}{\xi(\mathbf{Z})} \right)^{n(\mathbf{Z})} \left(\frac{n(\mathbf{Z}^c)}{\xi(\mathbf{Z}^c)} \right)^{n(\mathbf{Z}^c)} I\left(\frac{n(\mathbf{Z})}{\xi(\mathbf{Z})} > \frac{n(\mathbf{Z}^c)}{\xi(\mathbf{Z}^c)} \right) \quad (5)$$

where $\mathbf{Z}^c$ indicates all the regions outside the window $\mathbf{Z}$, and $n()$ denotes the observed number of cases within the specified window and $I()$ is the indicator function. The window $\mathbf{Z}^*$ that attains the maximum likelihood is defined as the *most likely cluster* (MLC). To find the distribution of the test statistic under the null hypothesis, Monte Carlo hypothesis testing [19] is required. In this paper, p-value of the test is based upon the null distribution of likelihood ratio test statistic with a large number (we used 999) of Monte Carlo replications of the data set generated under the null hypothesis. It should be noted that, in the same manner as the circular spatial scan statistic, the flexible spatial scan statistic is also able to locate secondary clusters that do not overlap the most likely cluster but are still statistically significant.

Results

Illustrations and powers

In this section, we will compare the flexible spatial scan statistic with the circular spatial scan statistic. As an entire study population, we will use $m = 113$ regions comprising the wards, cities and villages in the area of Tokyo Metropolis and Kanagawa prefecture in Japan (Figure 1). The variability of regional populations for $m = 113$ regions is: 25 percentile = 56, 704, median = 142, 320 and 75 percentile = 200, 936.

Hot-spot clusters

We will consider the following four hot-spot clusters where the expected total number of cases $\sum_{i=1}^{m} \xi_i$ is set to be 200 under the null hypothesis.

1. Cluster **A** = {14, 15, 20}

2. Cluster **B** = {14, 15, 20, 26}

3. Cluster **C** = {14, 15, 26, 27}

4. Cluster **D** = {73, 74, 75, 76, 78}

where the region included in a hot-spot cluster is called a "hot-spot region" (hot-spot region numbers are shown in Figure 1). The relative risk within any cluster **R** is set to three, i.e.,

$$H_1 : N(\mathbf{R}) \sim \text{Pois}(\theta\xi(\mathbf{R})), \; \theta = 3.0 \quad (6)$$

The cluster **A** is considered here as an example of a circular cluster that can be in the set of the circular windows and is expected to be identified by the circular spatial scan statistic more often than by the flexible spatial scan statistic. The other clusters are examples of noncircular clusters that are not in the set of the circular windows and thus cannot be identified correctly by the circular spatial scan statistics. For example, consider the region $i_0 = 15$ as the starting region and the set of $(K - 1)$-nearest neighbours to the region 15, which is listed as follows in the ascending order of distance from the region 15:

15, 14, 20, 12, 4, 26, 13, 27, 16, 40, 19, 42, 10,...,

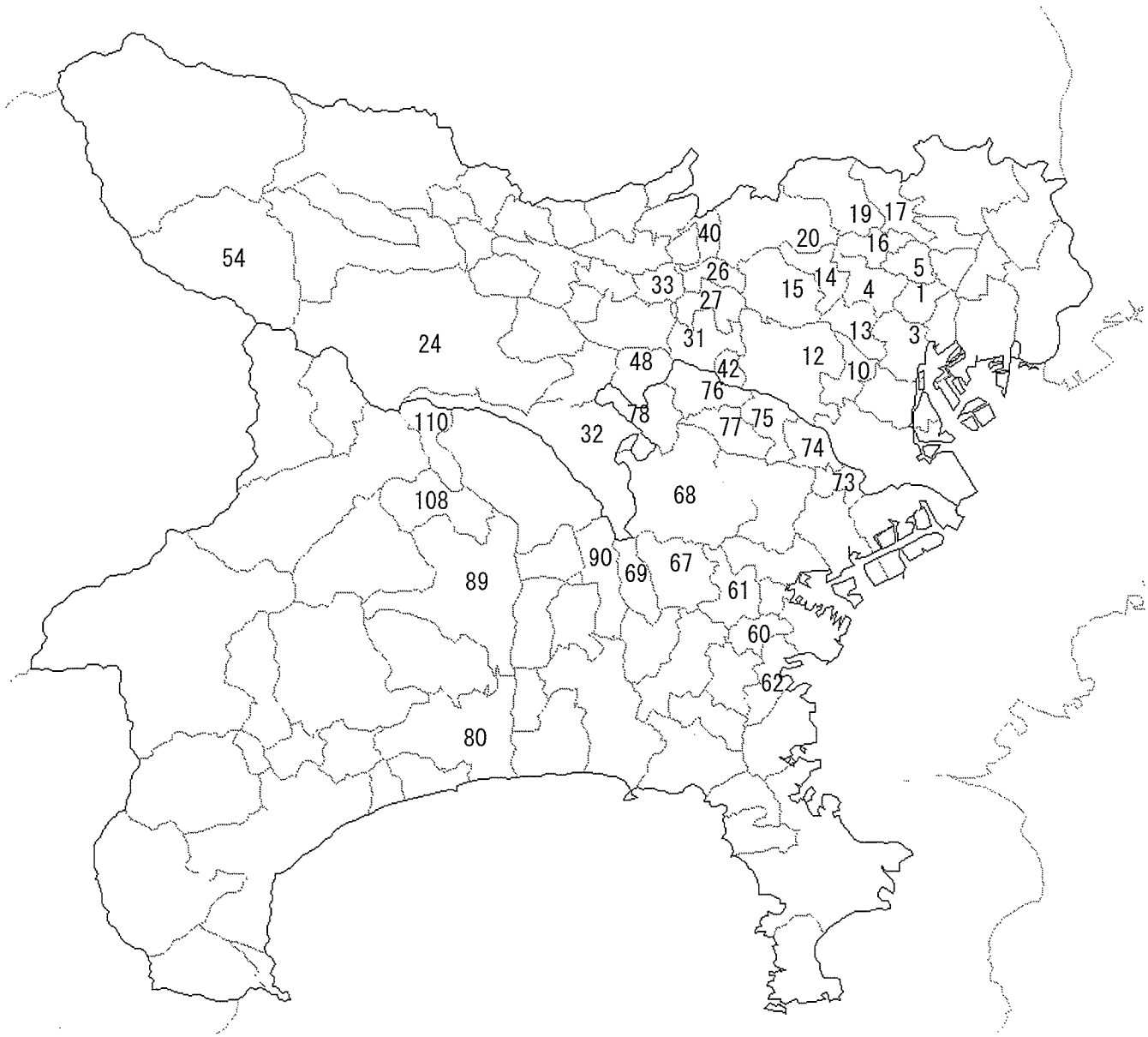

Figure 1

An entire study population for simulation studies. The 113 regions comprising wards, cities and villages in the area of Tokyo Metropolis and Kanagawa prefecture in Japan. The region number used in the text is shown. Especially, The region numbers of four hot-spot clusters **A-D** are **A** = {14, 15, 20}, **B** = {14, 15, 20, 26}, **C** = {14, 15, 26, 27}, and **D** = {73, 74, 75, 76, 78}, respectively.

In this case, circular windows are {15}, {15, 14}, {15, 14, 20}, {15, 14, 20, 12}, ... When the starting region is 14 or 20, the corresponding set of (K - 1)-nearest neighbours is

14, 15, 20, 4, 16, 13, 19, 12, 5, 1, 17, 10, 26, 3, 27,...,

and

20, 14, 15, 19, 16, 4, 17, 26, 40, 13, 5, 12, 1, 27,...,

respectively. In both cases, cluster B and C are easily found to be not in the set of circular windows. The cluster **D** is considered as an example of a long and narrow cluster as is shown in Figure 1.

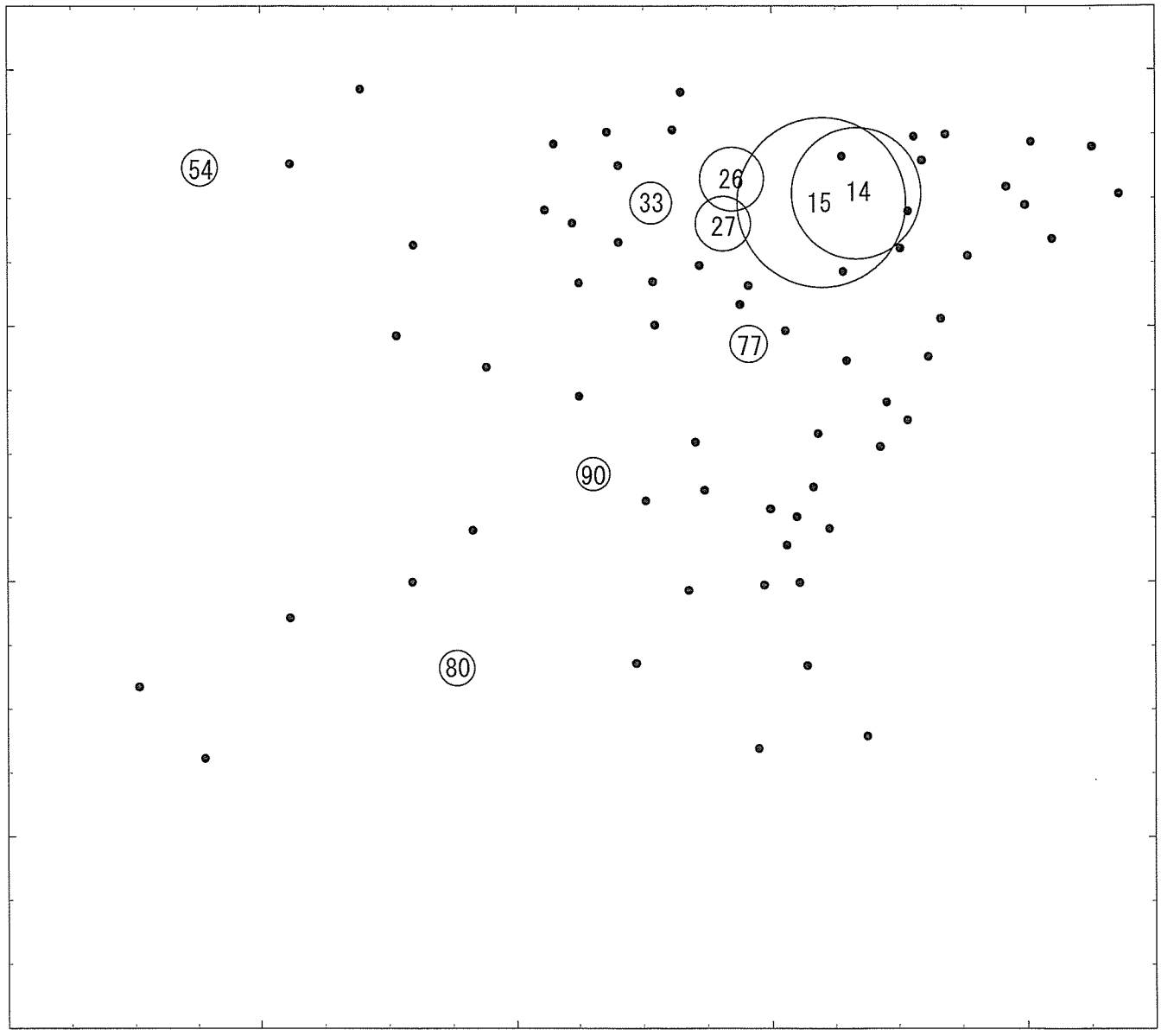

Figure 2
A random sample from cluster model C. Dots describe the centroids of regions with some cases. Circles are drawn only for the regions whose standardized risk ratios are statistically significantly larger than 1 at $\alpha = 0.05$ and the region number is placed in stead of dot. The radius is set inversely proportional to the tail probability.

Illustrative example

As an illustration, we will apply the circular spatial scan statistic, the flexible spatial scan statistic and Duczmal and Assunção's spatial scan statistic to the disease map shown in Figure 2 which is a random sample of $n = 235$ cases assuming the cluster model C. Circles are drawn only for the regions whose observed-expected ratio (standardized risk ratio) is statistically significantly larger than 1 at $\alpha = 0.05$. The radius of the circles is set inversely proportional to the upper tail p-value. The number shown in Figure 2 indicates the region number. Figure 2 obviously suggests the clusters occurring in the area including regions $\{14, 15, 26, 27, 33\}$.

Before applying the three spatial scan statistics, we have to specify a common maximum length K for the most likely cluster. This makes comparisons to a certain extent fair. In this example, we chose two kinds of maximum length $K =$

15 and $K = 20$ since it is not unreasonable to assume that an actual cluster size will be less than one third or one fourth of the size of the whole study area.

Irrespective of the value of K, the circular spatial scan statistic detected the regions {14, 15} as MLC with log likelihood ratio = 20.1, $p = 1/(999 + 1) = 0.001$ and the estimated relative risk is $\hat{\theta} = 3.47$. This is shown in Figure 3(a). The flexible spatial scan statistic, regardless of the value K, detected the regions {14, 15, 26, 27, 33} as MLC with log likelihood ratio = 29.7, $p = 0.001$ and the estimated relative risk is $\hat{\theta} = 3.41$. This is shown in Figure 3(b). Duczmal and Assunção's method, on the other hand, detected a cluster of peculiar shape that is much larger than the true cluster. In the case of $K = 15$, their scan statistic detected an area consisting of $K = 15$ connected regions {14, 15, 24, 26, 27, 31, 32, 33, 48, 54, 69, 77, 78, 90, 110 } as MLC with log likelihood ratio = 31.8, $p = 0.001$ and the estimated relative risk is $\hat{\theta} = 2.40$. This is shown in Figure 4(a). Figure 4(b) shows the most likely cluster {14, 15, 26, 27, 31, 32, 33, 48, 60, 61, 62, 67, 69, 77, 78, 80, 89, 90, 108, 110 } detected by Duczmal and Assunção's scan statistic for $K = 20$ where the length of MLC is also the same as $K = 20$ and log likelihood ratio = 36.0, $p = 0.001$ and the estimated relative risk is $\hat{\theta} = 2.26$. In the case of $K = 15$, the results of the three scan statistics are summarized in Table 1. Although the most likely cluster detected by Duczmal and Assunção's scan statistic has the largest log likelihood ratio among three scan statistics, it has detected MLC surprisingly larger than the true cluster.

Using a PC(Windows XP, CPU pentium 4, 3.2 GHz), the execution time of the flexible spatial scan statistic in this example is 14 seconds for $K = 15$ and 379 seconds for $K = 20$ which is certainly greater than that for the circular spatial scan statistic (less than 1 second for both $K = 15$ and $K = 20$).

Power comparison

In the power comparison, we chose $K = 15$. To compare the power of the flexible spatial scan statistic with that of the circular spatial scan statistic based upon Monte Carlo simulation, we will introduce a new bivariate power distribution $P(l, s)$ classified by the *length* l of the significant MLC and the number s of hot-spot regions included in the most likely cluster:

$$P(l,s) = \frac{\#\{\text{significant MLC has length } l \text{ and includes } s \text{ hot-spot regions}\}}{\#\{\text{trials for each simulation}\}}, \quad (7)$$

where $l \geq 1$ and $s \geq 0$. Based on $P(l, s)$, we examined the following powers,

1. the usual power, i.e., $P(+,+) = \sum_{l\geq 1} \sum_{s\geq 0} P(l, s)$,

2. the joint power $P(l, s)$, especially $P(s^*, s^*)$ where s^* is the length of the hot-spot cluster assumed in the simulation.

3. the marginal power distribution of $s(\geq 0)$, $P(+, s) = \sum_{l\geq 1} P(l, s)$ and its conditional power $P(+, s)/P(+,+)$,

4. the marginal power distribution of $l(\geq 1)$, $P(l, +) = \sum_{s\geq 0} P(l, s)$.

The powers are calculated for tests of nominal α levels of 0.05 and for the expected total number of cases 200 under the null hypothesis, which are based on Monte Carlo simulation using Poisson random numbers. For each simulation, 1,000 trials were carried out. The resultant power distribution $P(l, s) \times 1000$ is shown in Tables 2, 3, 4, 5 for each of the four cluster models, respectively, in the form of cross table classified by l ("*length*" in tables) and s ("*include*" in tables).

1) Usual power

Both tests have the same size 0.043 (distribution of length of significant MLC is omitted) and are shown to have high powers for the hot-spot clusters considered here. The flexible spatial scan statistic generally has higher power except for the model **A** (circular cluster) where, however, the difference is small.

2) Joint powers at (s, s*) and at its neighbours*

Table 2 shows the good characteristics of the circular spatial scan statistic. Namely, the circle-based scan statistic could detect circular hot-spot cluster **A** with length $s^* = 3$ considerably more accurately with power 738/1000 compared to 142/1000 of the flexible spatial scan statistic. Tables 3, 4, 5, on the other hand, show that the power of the circular spatial scan statistic in detecting exactly non-circular hot-spot clusters is 0/1000 due to the circular window. However, the circular spatial scan statistic is seen to be able to include some of the hot-spot regions into MLC reasonably well. For example, when applied to the non-circular cluster **B** with length $s^* = 4$, three or four regions including three hot-spot regions can be detected as the most likely cluster with relatively high power (523 + 65)/1000 = 0.588 (Table 3). When applied to the model **D** with length $s^* = 5$, the similar high power 363/1000 can be observed at $(l, s) = (6, 4)$ (Table 5). The flexible spatial scan statistic, on the other hand, has no such high power at a single point (l, s) near (s^*, s^*). However, the characteristic of the flexible spatial scan statistic is that the support of the power distribution is distributed in a relatively narrow range of l on the line $s = s^*$, i.e, we have $s^* \leq l \leq 12$ in the four cluster models considered here.

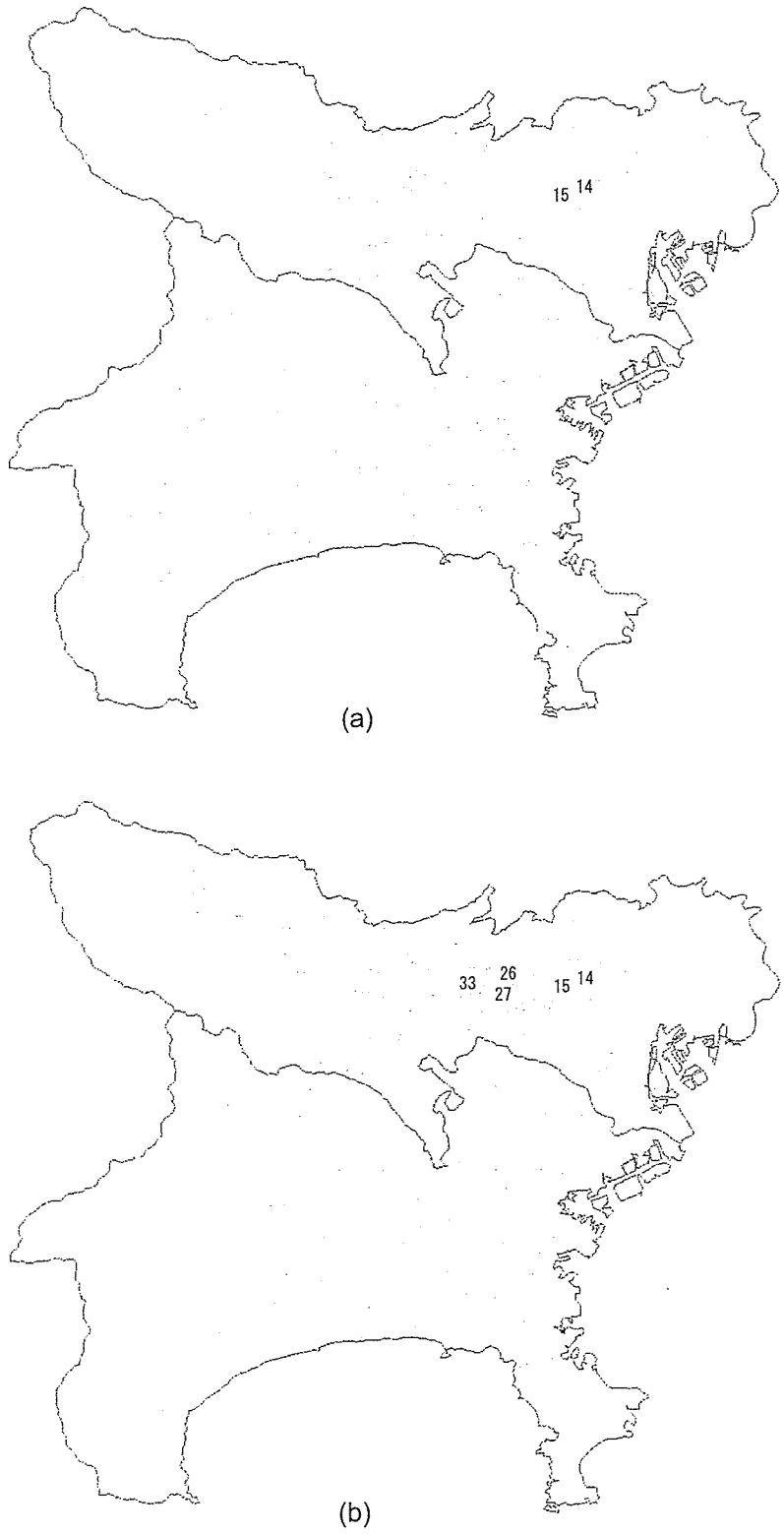

Figure 3
The most likely cluster detected by the circular and the flexible spatial scan statistic. (a) Detected by the circular spatial scan statistic for both $K = 15$ and $K = 20$ and (b) by the flexible spatial scan statistic for both $K = 15$ and $K = 20$, when applied to a random sample from the cluster model $\mathbf{C} = \{14, 15, 26, 27\}$.

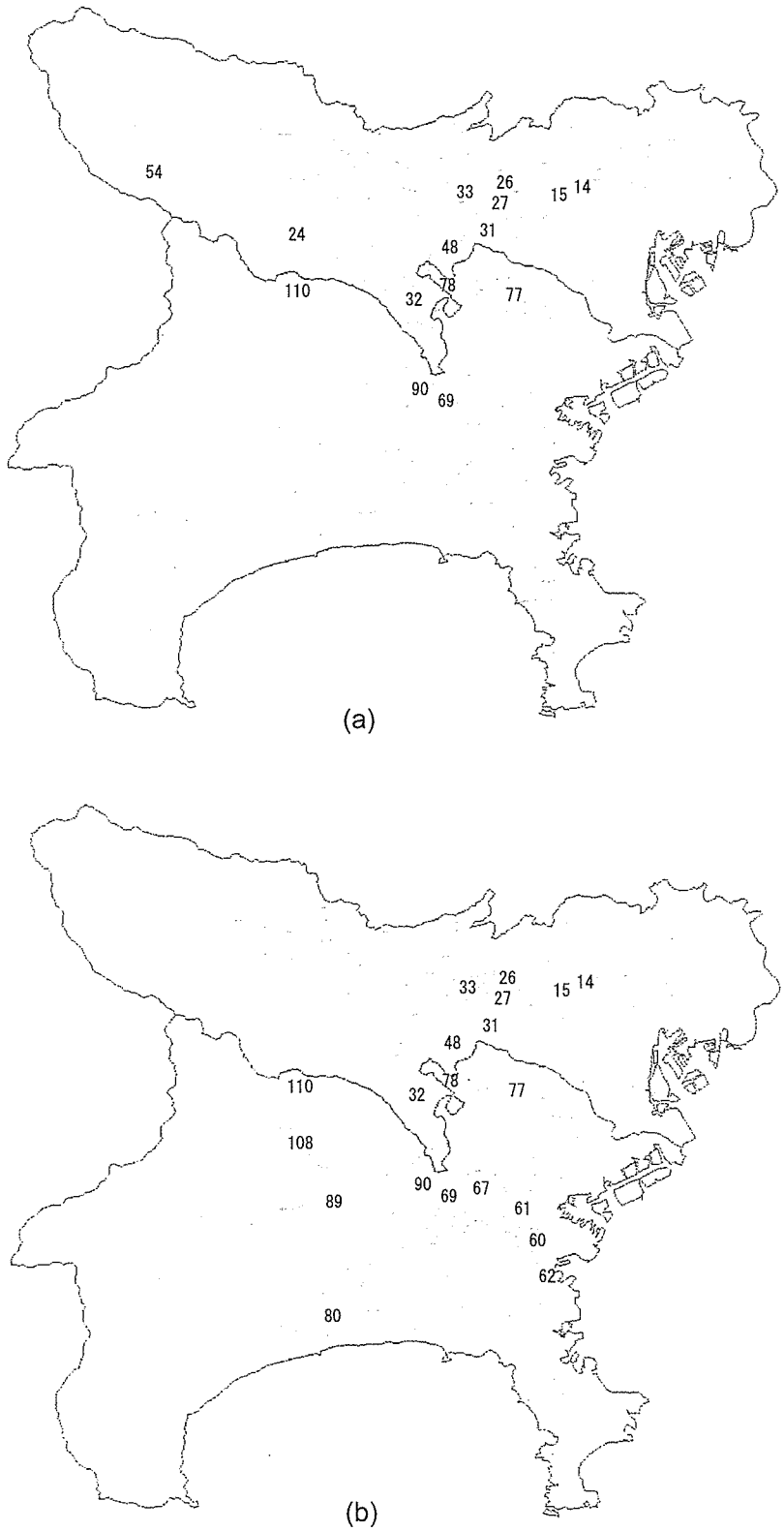

Figure 4
The most likely cluster detected by the Duczmal and Assunção's scan statistic. (a) Detected for $K = 15$ and (b) for $K = 20$, when applied to a random sample from the cluster model $\mathbf{C} = \{14, 15, 26, 27\}$.

Table 1: Regions detected as the most likely cluster by three procedures. Regions detected as the most likely cluster by the circular scan, the flexible scan and Duczmal and Assunção's scan, with the maximum length of cluster set to be $K = 15$ for the simulated random sample from the cluster model C where the hot spot cluster is assumed to be the set of connected four regions {14, 15, 26, 27} with the assumed relative risk $\theta = 3.0$. For details, see text.

region no.	population	observed no. cases	expected no. cases	relative risk estimated (true)	Log likelihood ratio (LLR) and estimated relative risk $\hat{\theta}$ for the most likely cluster		
					Circular	Flexible	Duczmal et al.
14	319,687	14	3.794	3.69 (3.0)	*	*	*
15	529,485	21	6.283	3.34 (3.0)	*	*	*
					LLR = 20.1		
					$\hat{\theta}$ = 3.47		
26	139,077	6	1.650	3.64 (3.0)		*	*
27	165,564	6	1.964	3.05 (3.0)		*	*
33	105,899	4	1.257	3.18 (1.0)		*	*
						LLR = 29.7	
						$\hat{\theta}$ = 3.41	
24	466,347	8	5.534	1.44 (1.0)			*
31	197,677	3	2.346	1.27 (1.0)			*
32	349,050	5	4.142	1.20 (1.0)			*
48	58,635	1	0.696	1.43 (1.0)			*
54	3,808	1	0.045	22.12(1.0)			*
69	119,575	3	1.419	2.11 (1.0)			*
77	177,742	5	2.109	2.37 (1.0)			*
78	125,127	2	1.485	1.34 (1.0)			*
90	194,866	5	2.312	2.16 (1.0)			*
110	21,535	1	0.256	3.91 (1.0)			*
							LLR = 31.8
							$\hat{\theta}$ = 2.41

3) Marginal power P(+, s) and its conditional marginal power P(+, s)/P(+, +)

Regarding the marginal power $P(+, s^*)$ at $s = s^*$, the flexible spatial scan statistic is shown to have much higher power than the circular spatial scan statistic for the case of noncircular clusters (Tables 3, 4, 5). Furthermore, the conditional marginal power $P(+, s)/P(+, +)$ of the flexible spatial scan statistic is 964/964 = 1.000, 969/979 = 0.990, 850/890 = 0.955 and 612/673 = 0.909 for the cluster **A-D**, respectively. These results indicate that the identified MLC by the flexible spatial scan statistic includes the hot-spot cluster with quite high probability. For the noncircular clusters, the mode of $P(+, s)$ of the circular spatial scan statistic is around $s = s^* - 1$ or $s = s^* - 2$.

4) Marginal power distribution P(l, +)

For the flexible spatial scan statistic, the probability that the length of significant MLC is less than $s = s^*$ is shown to be zero or quite small and the maximum length is around 10 to 12. the circular spatial scan statistic, on the other hand, tends to detect a much longer cluster than expected from the hot-spot cluster assumed in the simulation. For example, the probability that the length of MLC for the cluster B with length $s^* = 4$ is greater than or equal

Table 2: Comparison of the circular and the flexible spatial scan statistic for the cluster model A. Comparison of bivariate power distribution $P(l, s) \times 1000$ between the circular spatial scan statistic and the flexible spatial scan statistic for the hot-spot cluster A = {14, 15, 20}. Nominal α-level is set as 0.05 and 1000 trials are carried out. For more details, see text.

Flexible (K = 15)						Circular (K = 15)					
Length l	Include s hot-spot regions				Total	Length l	Include s hot-spot regions				Total
	0	1	2	3			0	1	2	3	
1	0	0			0	1	0	0			0
2	0	0	0		0	2	1	0	0		1
3	0	0	0	142	142	3	0	0	0	738	738
4	0	0	0	116	116	4	0	0	0	134	134
5	0	0	0	137	137	5	0	0	0	39	39
6	0	0	0	149	149	6	0	0	0	12	12
7	0	0	0	165	165	7	0	0	0	9	9
8	0	0	0	131	131	8	0	0	0	1	1
9	0	0	0	84	84	9	0	0	2	3	5
10	0	0	0	27	27	10	0	0	0	2	2
11	0	0	0	11	11	11	0	0	0	4	4
12	0	0	0	2	2	12	0	0	0	12	12
13	0	0	0	0	0	13	0	0	0	14	14
14	0	0	0	0	0	14	0	0	0	3	3
15	0	0	0	0	0	15	0	0	0	6	6
Total	0	0	0	964	964	Total	1	0	2	977	980
		usual power = 0.964						usual power = 0.980			

Table 3: Comparison of the circular and the flexible spatial scan statistic for the cluster model B. Comparison of bivariate power distribution $P(l, s) \times 1000$ between the circular spatial scan statistic and the flexible spatial scan statistic for the hot-spot cluster B = {14, 15, 20, 26}. Nominal α-level is set as 0.05 and 1000 trials are carried out. For more details, see text.

Flexible (K = 15)							Circular (K = 15)						
Length l	Include s hot-spot regions					Total	Length l	Include s hot-spot regions					Total
	0	1	2	3	4			0	1	2	3	4	
1	0	0				0	1	0	0				0
2	0	0	0			0	2	0	0	0			0
3	0	0	0	0		0	3	0	0	0	523		523
4	0	0	0	0	127	127	4	0	0	0	65	0	65
5	1	0	0	0	157	158	5	0	0	0	23	0	23
6	0	0	0	0	205	205	6	0	0	0	7	66	73
7	0	0	0	2	198	200	7	0	0	0	0	15	15
8	0	0	0	1	151	152	8	0	0	0	0	32	32
9	0	0	0	5	85	90	9	0	0	0	1	15	16
10	0	0	0	1	24	25	10	0	0	0	0	7	7
11	0	0	0	0	17	17	11	0	0	0	2	3	5
12	0	0	0	0	5	5	12	0	0	0	2	63	65
13	0	0	0	0	0	0	13	0	0	0	0	96	96
14	0	0	0	0	0	0	14	0	0	0	0	30	30
15	0	0	0	0	0	0	15	0	0	0	0	22	22
Total	1	0	0	9	969	979	Total	0	0	0	623	349	972
			usual power = 0.979							usual power = 0.972			

Table 4: Comparison of the circular and the flexible spatial scan statistic for the cluster model C. Comparison of bivariate power distribution $P(l, s) \times 1000$ between the circular spatial scan statistic and the flexible spatial scan statistic for the hot-spot cluster C = {14, 15, 26, 27}. Nominal α-level is set as 0.05 and 1000 trials are carried out. For more details, see text.

Flexible (K = 15)							Circular (K = 15)						
Length l	Include s hot-spot regions					Total	Length l	Include s hot-spot regions					Total
	0	1	2	3	4			0	1	2	3	4	
1	0	0				0	1	1	0				1
2	0	0	0			0	2	0	0	351			351
3	0	0	0	0		0	3	2	0	4	0		6
4	0	0	0	0	138	138	4	0	0	3	0	0	3
5	0	0	0	3	147	150	5	2	0	2	0	0	4
6	1	0	0	2	200	203	6	1	0	0	0	0	1
7	0	1	0	4	147	152	7	0	0	0	81	0	81
8	0	0	2	9	107	118	8	0	0	10	18	38	66
9	0	0	0	10	71	81	9	0	0	2	0	26	28
10	1	0	2	5	28	36	10	0	0	0	29	3	32
11	0	0	0	0	10	10	11	0	0	1	13	1	15
12	0	0	0	0	2	2	12	0	0	2	4	60	66
13	0	0	0	0	0	0	13	0	0	0	5	62	67
14	0	0	0	0	0	0	14	0	0	0	10	27	37
15	0	0	0	0	0	0	15	0	0	0	6	37	43
Total	2	1	4	33	850	890	Total	6	0	375	166	254	801
		usual power = 0.890							usual power = 0.801				

Table 5: Comparison of the circular and the flexible spatial scan statistic for the cluster model D. Comparison of bivariate power distribution $P(l, s) \times 1000$ between the circular spatial scan statistic and the flexible spatial scan statistic for the hot-spot cluster D = {73, 74, 75, 76, 78}. Nominal α-level is set as 0.05 and 1000 trials are carried out. For more details, see text.

Flexible (K = 15)								Circular (K = 15)							
Length l	Include s hot-spot regions						Total	Length l	Include s hot-spot regions						Total
	0	1	2	3	4	5			0	1	2	3	4	5	
1	0	0					0	1	6	0					6
2	1	0	0				1	2	3	5	0				8
3	0	0	0	0			0	3	0	0	0	14			14
4	1	0	0	1	0		2	4	1	0	4	5	0		10
5	0	1	0	3	1	242	247	5	0	0	2	1	0	0	3
6	1	0	0	1	2	162	166	6	1	0	0	1	363	0	365
7	2	3	0	5	5	93	108	7	0	0	1	0	56	0	57
8	1	2	1	6	7	53	70	8	0	0	2	2	28	0	32
9	0	2	0	1	5	38	46	9	0	0	2	2	10	0	14
10	0	2	0	1	1	18	22	10	1	0	0	3	3	0	7
11	0	0	0	2	2	5	9	11	0	0	0	0	3	11	14
12	0	0	1	0	0	1	2	12	0	0	0	2	3	8	13
13	0	0	0	0	0	0	0	13	0	0	0	1	1	16	18
14	0	0	0	0	0	0	0	14	0	0	1	0	0	5	6
15	0	0	0	0	0	0	0	15	0	1	0	0	1	7	9
Total	6	10	2	20	23	612	673	Total	12	6	12	31	468	47	576
			usual power = 0.673								usual power = 0.576				

Table 6: Cost comparison Expected number of undetected regions included in the true cluster $E(s^* - S)$, expected number of detected regions not in the true cluster $E(L - S)$ and the ratio of costs C/C_2 (r = 1, 2) incurred by incomplete identification of the true cluster. The spatial scan statistic with low values is better.

Hot-spot Cluster	Scan statistic	$E(s^* - S)$	$E(L - S)$	the ratio C/C_2	
				r = 1	r = 2
A = {14, 15, 20}	Flexible (K = 15)	0.108	2.951	3.059	3.167
	Circular (K = 15)	0.065	0.722	0.787	0.852
B = {14, 15, 20, 26}	Flexible (K = 15)	0.097	2.548	2.645	2.742
	Circular (K = 15)	0.735	2.525	3.260	3.995
C = {14, 15, 26, 27}	Flexible (K = 15)	0.492	2.243	2.735	3.227
	Circular (K = 15)	1.736	3.153	4.889	6.625
D = {73, 74, 75, 76, 78}	Flexible (K = 15)	1.774	1.088	2.862	4.636
	Circular (K = 15)	2.770	1.709	4.479	7.249

to 12 is 213/1000 = 0.213 compared with 5/1000 = 0.005 for the flexible spatial scan statistic. The probability that the length of MLC for the cluster **C** with length $s^* = 4$ is greater than or equal to 12 is 213/1000 = 0.213 compared with 2/1000 = 0.002 for the flexible spatial scan statistic. This tendency is shown even in the circular cluster **A** where the same probabilities are 0.035 vs. 0.002.

Cost comparison

Based upon the bivariate power function $P(l, s)$, we can compute the following expected total cost incurred by incomplete identification of the true cluster:

$$C = C_2\{rE(s^* - S) + E(L - S)\}, r = C_1/C_2 \quad (8)$$

where C_1 and C_2 denote the average cost of missing one region in the true cluster and that of incorrectly detecting one region not in the true cluster, respectively. L and S denote the random variable of l and s, respectively. Two expected numbers $E(s^* - S)$ and $E(L - S)$ for four kinds of clusters **A-D** are shown in Table 6. In general, we can assume $r > 1$. For example, the ratio C/C_2 is shown for the case of $r = 1$ and $r = 2$, respectively, in Table 6. However, in this example, irrespective of the value of $r(> 1)$, the circular spatial scan statistic is shown to have lower cost for detecting circular cluster **A** but to have higher cost for detecting non-circular clusters **B-D**.

Limitations of current work

Needless to say, the results derived here are based upon a small Monte Carlo simulations study and thus the characteristic observed in the current work could change a little bit depending on the cluster model adopted. We assumed here only one hot spot cluster and did not consider the case of several hot spot clusters. Therefore, we need a further simulation study to compare the performance of the two spatial scan statistics under several different clusters.

Regarding the algorithm adopted for the flexible spatial scan statistic, we set the restriction that irregularly shaped windows **Z** with length $k(\leq K)$ are constructed from members of the $(K - 1)$-nearest neighbours to the starting region. It seems that this restriction plays an important role in preventing the flexible spatial scan statistic from reaching out for and absorbing faraway regions with non-elevated risk. However, to avoid undertaking computationally infeasible searches, the flexible spatial scan statistic has to be set with an upperbound for K. This depends on the disease map under study and the capability of the computer. The current practical upperbound is around $K = 30$ for the reason that the execution time of our current algorithm will take more than a week if $K > 30$ for the number of regions $m = 200 \sim 300$. However, it seems to be unlikely that the length of the true cluster would be larger than $10 \sim 15$ percent of the total number of regions. So, we think that our current algorithm can be applied to many epidemiological studies with small to moderate cluster sizes. However, for larger cluster sizes, a more sophisticated algorithm to increase the upperbound for K is needed.

Regarding data type, the proposed spatial scan statistic can only be applied to regional count data whereas the circular spatial scan statistic can be applied to not only count data but also individual point data. However, at least in disease surveillance, most of the data that people

analyze is aggregated, so the method covers most real-world situations.

Finally, one of the reviewers commented that using small areas as basis for clustering without any attempt to incorporate heterogeneity in background rates is a fundamental flaw of all existing scanning methods. In general, we know that disease risks over study regions are heterogeneous to a certain extent and the null hypothesis of complete spatial randomness is not true. However, statistical hypothesis testing is based upon the null hypothesis which is not true. Likewise, we will use complete spatial randomness as the null hypothesis as indicated in equation (1) since we are interested in rejecting the null hypothesis and detecting the local clusters with excess risk. If we are interested in estimating a clustering mechanism, we should use some modeling approach rather than spatial scan statistics.

Discussion

In this paper, we proposed a flexibly shaped spatial scan statistic to detect arbitrarily shaped clusters by amalgamating administrative units. The flexible spatial scan statistic is, via Monte Carlo simulation, shown to have reasonably high powers compared with the circular spatial scan statistic when examined by a newly introduced bivariate power distribution $P(l, s)$. The simulation reveals that the circular spatial scan statistics shows a high level of accuracy in detecting circular clusters exactly and reasonably good power for including some hot-spot regions into the most likely cluster. The flexible spatial scan statistic exhibits no such high power regarding exact identification of clusters but the support of the power distribution is shown to be concentrated in a relatively narrow range of length l on the line $s = s^*$, indicating that an observed significant most likely cluster contains the true cluster with quite high probability. The circular spatial scan statistic, on the other hand, is shown to have zero powers for detecting exactly noncircular clusters that cannot be captured by any circular window. The circular spatial scan statistic is also shown to have a tendency to detect a larger cluster than the true cluster assumed in the simulation even for the case when the true cluster is circular. Furthermore, by introducing the two kinds of cost due to incomplete detection of the true cluster, we could summarize these characteristics in terms of minimizing expected total cost. One of the reviewers suggested a similar cost comparison using the number of people that are incorrectly classified rather than the number of regions since the cost of misclassifying a large region is at least for disease surveillance purposes higher than that of misclassifying a region with smaller population. We think that would be an interesting additional simulation study worth conducting. However, since it can be expected that the result of such a cost comparison strongly depends on the spatial configuration of regions with different population size in the neighborhood of and within the true cluster and thus it requires careful design for creating suitable cluster models from which we can intuitively infer the result to a certain extent, we would like to leave such a simulation study in our future work.

The surprising result that Duczmal and Assunção's scan statistic detected quite large and unlikely peculiar shaped clusters that had the largest likelihood ratio among the three scan statistics might cast a doubt on the validity of the model selection based upon maximizing the likelihood ratio (5). Such a doubt can also be seen in some simulation results of the circular spatial scan statistic that had non-negligible probabilities of detecting much longer clusters than the true cluster. The flexible spatial scan statistic, on the other hand, is shown not to detect such an unexpected long cluster probably because it has the restriction that our windows are constructed only from members of the $(K - 1)$-nearest neighbours to the starting region. Nevertheless, these undesirable properties produced by maximum likelihood ratio might suggest the use of a different criterion for model selection. For example, we might consider a penalized likelihood where we consider a penalty for the *complexity of the cluster shape*, which is also worth future research.

All the computations and simulations have been conducted on a PC with Windows XP. For users who are interested in applying the flexible spatial scan statistic, we can provide the software FleXScan [20].

Conclusion

The circular spatial scan statistics shows a high level of accuracy in detecting circular clusters exactly and reasonably good power for including some hot-spot regions into the most likely cluster. The proposed flexible spatial scan statistic is shown to have good usual powers plus the ability to detect the noncircular hot-spot clusters more accurately than the circular spatial scan statistic. However, the proposed spatial scan statistic work well for small to moderate cluster size, say up to 30. For larger cluster sizes, the method is not practically feasible and a more efficient algorithm is needed.

Appendix: algorithm to find the set Z_2 defined in equation (3)

There are probably several procedures to find the set Z_2 that is defined as the set of arbitrarily shaped windows $\mathbf{Z}$ within a pre-specified maximum length K. The algorithm that we used is described as follows:

Step 1. First we set an $m \times m$ matrix $A = (a_{ij})$ such as

$$a_{ij} = \begin{cases} 1 & \text{(regions } i \text{ and } j \text{ are connected)} \\ 0 & \text{(otherwise),} \end{cases}$$

and set $Z_2 = \phi$ and $i_0 = 0$

Step 2. Let $i_0 \leftarrow i_0 + 1$ and $i_0 (= 1, 2, \ldots, m)$ be the starting region. Then we create the set W_{i_0} consisting of $(K - 1)$-nearest neighbours to the starting region i_0 and i_0 itself, i.e.,

$$W_{i_0} = \{i_0, i_1, i_2, \ldots, i_{K-1}\},$$

where i_k is the k-th nearest to i_0.

Step 3. We consider all the set $Z \subset W_{i_0}$, which includes the starting region i_0. For any given such set Z, repeat the following steps 4–7.

Step 4. We divide the set Z into two disjoint sets: $Z_0 = \{i_0\}$ and Z_1 which contains the other regions of Z.

Step 5. We make two new sets $\mathbf{Z}_0'$ and $\mathbf{Z}_1'$. $\mathbf{Z}_0'$ consists of the regions of Z_1 that are connected to some regions of Z_0. On the other hand, $\mathbf{Z}_1'$ consists of the regions of Z_1 that are not connected to any regions of Z_0. Then we replace Z_0 and Z_1 by $\mathbf{Z}_0'$ and $\mathbf{Z}_1'$, respectively.

Step 6. We repeat the step 5 recursively until either Z_0 or Z_1 becomes null first.

Step 7. We make a decision as follows. Z is said to be "connected" when Z_1 becomes null first and "disconnected" when Z_0 becomes null first. If we can find Z "connected", Z is added to the set Z_2. If we find Z "disconnected", Z is discarded.

Step 8. Repeat the steps 2–7 until we finally get the set Z_2 consisting of arbitrarily shaped windows Z whose maximum length is K.

Now we shall give an example using regions in the Tokyo Metropolitan area shown in Figure 1. Let the starting region $i_0 = 14$. Then, the regions in the set of $(K - 1)$-nearest neighbours to the region 14 are listed as follows in the ascending order of distance to the region 14, i.e.,

$$W_{14} = \{14, 15, 20, 4, 16, 13, 19, 12, 5, \ldots\}.$$

Suppose that we take a subset $Z = \{14, 15, 20, 26\}$. In the first step, we have

$$Z_0 = \{14\}, Z_1 = \{15, 20, 26\}.$$

Since $a_{14,15} = a_{14,20} = 1$ and $a_{14,26} = 0$, we then have

$$Z_0 = \{15, 20\}, Z_1 = \{26\}.$$

Further, because $a_{15,26} = a_{20,26} = 1$, these sets are replaced by

$$Z_0 = \{26\}, Z_1 = \phi.$$

So, we can find that the set $Z = \{14, 15, 20, 26\}$ is "connected" and can be a member of Z_2.

If we take a subset $Z = \{14, 15, 20, 5\}$, we can find Z is "disconnected" because $a_{14,5} = a_{15,5} = a_{20,5} = 0$, $Z_0 = \phi$ and $Z_1 = \{5\}$ at the final stage.

Authors' contributions

TT proposed the flexibly shaped spatial scan statistic and the bivariate power distribution. KT considered the algorithm given in the appendix, programmed the C++ code and carried out the power simulations. TT wrote the first draft of the manuscript. Both authors interpreted the results and wrote the final version of the paper.

Acknowledgements

This research was supported in part by Grant-in-Aid for Scientific Research (Grant No. 16300091) from the Ministry of Education, Culture, Sports, Science and Technology of Japan.

References

1. Marshall RJ: **A review of the statistical analysis of spatial patterns of disease.** *Journal of Royal Statistical Society, Series A* 1991, **154:**421-441.
2. Lawson A, Biggeri A, Böhning D, Lesaffre E, Viel JF, Bertollini R, (Eds): *Disease Mapping and Risk Assessment for Public Health* London: John Wiley & Sons; 1999.
3. Lawson A, Denison D: *Spatial Cluster Modelling* Boca Raton: CRC Press; 2002.
4. Waller LA, Gotway CA: *Applied Spatial Statistics for Public Health Data* New York: John Wiley & Sons; 2004.
5. Cuzick J, Edwards R: **Spatial clustering for inhomogeneous populations (with discussion).** *Journal of the Royal Statistical Society, Series B* 1990, **52:**73-104.
6. Besag J, Newell J: **The detection of clusters in rare diseases.** *Journal of the Royal Statistical Society, Series A* 1991, **154:**143-155.
7. Kulldorff M, Nagarwalla N: **Spatial disease clusters: detextion and inference.** *Statistics in Medicine* 1995, **14:**799-810.
8. Kulldorff M: **A spatial scan statistic.** *Communications in Statistics* 1997, **26:**1481-1496.
9. Tango T: **A class of tests for detecting 'general' and 'focused' clustering of rare diseases.** *Statistics in Medicine* 1995, **14:**2323-2334.
10. Tango T: **A test for spatial disease clustering adjusted for multiple testing.** *Statistics in Medicine* 2000, **19:**191-204.
11. Viel JF, Arveux P, Baverel J, Cahn JY: **Soft-tissue sarcoma and non-Hodgkin's lymphoma clusters and a municipal solid waste incinerator with high dioxin emission levels.** *American Journal of Epidemiology* 2000, **152:**13-19.
12. Sankoh OA, Ye Y, Sauerborn R, Muller O, Becher H: **Clustering of childhood mortality in rural Burkina Faso.** *International Journal of Epidemiology* 2001, **30:**485-492.
13. Perez AM, Ward MP, Torres P, Ritacco V: **Use of spatial scan statistics and monitoring data to identifyclustering of bovine**

tuberculosis in Argentina. *Preventive Veterinary Medicine* 2002, **56:**63-74.
14. Kulldorff M, Tango T, Park PJ: **Power comparisons for disease clustering tests.** *Computational Statistics and Data Analysis* 2003, **42:**665-684.
15. Song C, Kulldorff M: **Power evaluation of disease clustering tests.** *International Journal of Health Geographics* 2003, **2(9):**1-8.
16. Kulldorff M, Information Management Services Inc: **SaTScan v4.0: Software for the spatial and space-time scan statistics.** 2004 [http://www.satscan.org/].
17. Patil GP, Taillie C: **Upper level set scan statistic for detecting arbitrarily shaped hotspots.** *Environmental and Ecological Statistics* 2004, **11:**183-197.
18. Duczmal L, Assunção R: **A simulated annealing strategy for the detection of arbitrarily shaped spatial clusters.** *Computational Statistics & Data Analysis* 2004, **45:**269-286.
19. Dwass M: **Modified randomization test for nonparametric hypotheses.** *Annals of Mathematical Statistics* 1957, **28:**181-187.
20. Takahashi K, Yokoyama T, Tango T: **FleXScan: Software for the flexible spatial scan statistic.** National Institute of Public Health, Japan; 2004.